PLATELETS AND THROMBOPOIESIS

SDF-1 dynamically mediates megakaryocyte niche occupancy and thrombopoiesis at steady state and following radiation injury

Lisa M. Niswander,[1,2] Katherine H. Fegan,[1] Paul D. Kingsley,[1] Kathleen E. McGrath,[1] and James Palis[1]

[1]Center for Pediatric Biomedical Research, Department of Pediatrics, and [2]Department of Pathology and Laboratory Medicine, University of Rochester Medical Center, Rochester, NY

Key Points

- SDF-1 acutely affects megakaryocyte spatial distribution in the bone marrow at steady state and in the setting of radiation injury.
- SDF-1-directed localization of megakaryocytes into the vascular niche increases platelet output.

Megakaryocyte (MK) development in the bone marrow progresses spatially from the endosteal niche, which promotes MK progenitor proliferation, to the sinusoidal vascular niche, the site of terminal maturation and thrombopoiesis. The chemokine stromal cell-derived factor-1 (SDF-1), signaling through CXCR4, is implicated in the maturational chemotaxis of MKs toward sinusoidal vessels. Here, we demonstrate that both IV administration of SDF-1 and stabilization of endogenous SDF-1 acutely increase MK-vasculature association and thrombopoiesis with no change in MK number. In the setting of radiation injury, we find dynamic fluctuations in marrow SDF-1 distribution that spatially and temporally correlate with variations in MK niche occupancy. Stabilization of altered SDF-1 gradients directly affects MK location. Importantly, these SDF-1-mediated changes have functional consequences for platelet production, as the movement of MKs away from the vasculature decreases circulating platelets, while MK association with the vasculature increases circulating platelets. Finally, we demonstrate that manipulation of SDF-1 gradients can improve radiation-induced thrombocytopenia in a manner additive with earlier TPO treatment. Taken together, our data support the concept that SDF-1 regulates the spatial distribution of MKs in the marrow and consequently circulating platelet numbers. This knowledge of the microenvironmental regulation of the MK lineage could lead to improved therapeutic strategies for thrombocytopenia. (*Blood*. 2014;124(2):277-286)

Introduction

Platelet-producing megakaryocytes (MKs) are derived from megakaryocyte progenitors (MKPs), which are defined functionally by their capacity to form colonies in vitro.[1,2] MKPs are thought to reside near the bone surface in an "endosteal niche," where environmental cues encourage expansion, but suppress terminal maturation.[3-6] Polyploid MKs mature cytoplasmically, extrude proplatelets in association with sinusoidal vasculature, and shed platelets into the peripheral blood.[7-9] This process results in past-maturity "exhausted" MKs comprised of a nucleus with a thin layer of cytoplasm surrounded by a cell membrane.[10,11] Megakaryopoiesis is primarily regulated by the cytokine thrombopoietin (TPO), which signals through its receptor Mpl to promote MKP proliferation and MK maturation.[12-14]

Although the physical association of MKs with sinusoidal vasculature was first appreciated several decades ago,[15-17] the functional significance of the "vascular niche" for MK maturation and thrombopoiesis has only more recently begun to be elucidated.[4,18-21] Several studies have implicated the chemokine stromal cell-derived factor-1 ([SDF-1] or CXCL12) signaling through receptor CXCR4 in the maturational localization of MKs to the vascular niche. CXCR4 is expressed throughout the MK lineage, and in vitro SDF-1 stimulation results in intracellular calcium mobilization, matrix metalloproteinase 9 expression, surface CXCR4 polarization, and ultimately migration along an SDF-1 gradient.[22-27] Several cell types within the bone marrow produce SDF-1, including osteoblasts, endothelial cells, and perivascular mesenchymal stromal cell populations.[28-32] Additionally, in vivo studies demonstrate that sustained elevation of SDF-1 in the blood increases thrombopoiesis, with images indicating enhanced MK association with vasculature.[20,33] Recently, VEGF-A treatment was shown to increase MK-vasculature interactions in vivo through upregulation of CXCR4 on MKs.[34] Despite this growing body of evidence indicating a role for SDF-1/CXCR4 in megakaryopoiesis, the acute and endogenous effects of SDF-1 on MK localization and platelet production remain unknown.

Radiation causes significant damage to the hematopoietic system, and thrombocytopenia can be a life-threatening consequence of radiation exposure.[35] Seminal studies in rodents identified an initial persistence of polyploid MKs after both sublethal and lethal doses of total body irradiation (TBI).[36-39] Accordingly, radioresistant MKs persist within an injured marrow microenvironment established by differential radiation damage to surrounding cell populations.[40-43] The sinusoidal vasculature, which supports platelet production, can dilate as surrounding cells succumb to damage and become leaky at higher levels of injury.[44,45] Intriguingly, SDF-1 levels increase in the marrow after TBI and radioresistant MKs relocate to the endosteal niche.[39,46,47] It is not known whether the spatial changes of MKs in the setting of TBI are regulated

Submitted January 8, 2014; accepted April 3, 2014. Prepublished online as *Blood* First Edition paper, April 15, 2014; DOI 10.1182/blood-2014-01-547638.

The online version of this article contains a data supplement.

There is an Inside *Blood* Commentary on this article in this issue.

The publication costs of this article were defrayed in part by page charge payment. Therefore, and solely to indicate this fact, this article is hereby marked "advertisement" in accordance with 18 USC section 1734.

by microenvironmental changes in SDF-1 or have functional consequences for platelet production.

Here, we investigate the ability of SDF-1 to acutely control MK location in the bone marrow both at steady state and after radiation injury. Importantly, we demonstrate that endogenous SDF-1 regulates the association of MKs with vasculature, which contributes to platelet production in uninjured bone marrow. After sublethal TBI, fluctuations in marrow SDF-1 dynamically affect the distribution of MKs. Our data give insight into the spatial regulation of megakaryopoiesis and demonstrate that changes in MK location have functional consequences for thrombopoiesis.

Materials and methods

Mice and irradiation

Seven- to 9-week-old female C57BL/6J mice (Jackson Laboratory) were used for all experiments. Unanesthetized mice, confined in a Plexiglass restraint, were exposed to 4 Gy TBI at a dose rate of 1.6 Gy/min using a Shephard Irradiator with 6000 Ci ^{137}Cs source and collimating equipment. All animal experiments were approved by the University of Rochester Committee on Animal Resources.

In vivo treatments

Recombinant murine SDF-1a (400 ng; Peprotech) in 100 μL phosphate-buffered saline (PBS) was injected IV into unirradiated mice, or mice at day 2 or day 4 post-TBI. Diprotin A ([ILE-PRO-ILE]; 1.7mg; Enzo) in 250 μL PBS was injected intraperitoneally into unirradiated mice, or mice at day 2 or day 3 post-TBI. Recombinant murine TPO (0.3μg; Peprotech) in 250 μl PBS was injected intraperitoneally 2 hours after 4 Gy TBI.

Blood and marrow isolation

Mice were killed by CO_2 narcosis and peripheral blood collected from the inferior vena cava. Femoral marrow was flushed into PB2[48] with 25 μg/mL heparin and titurated cells counted by hemocytometer.

MK lineage analysis

Platelet counts were obtained using a HemaTrue Veterinary Hematology Analyzer (Heska). For platelet RNA analysis, EDTA-collected blood was stained in PBS with 1000 U/mL heparin, 1 μg/mL thiozole orange (Sigma-Aldrich), and 1:100 eFluor450-CD41 and phycoerythrin (PE) Cy7-Ter119 (eBioscience), fixed with 1% formaldehyde, and analyzed by Imagestream^X (Amnis).

MKPs were quantified by colony assay, as previously described.[49] MK analysis was performed by imaging flow cytometry, as recently described.[50] PE-CXCR4 (eBioscience) was used to determine median fluorescent intensity per unit area (MFI/A) for each individual MK with the median pixel intensity feature (IDEAS [version 4.0]; Amnis).

In vitro differentiation of MKs

Marrow cells were stained with biotinylated Kit antibody (EBioscience), incubated with IMag streptavidin magnetic particles, and magnetically separated (iMagnet; BD Biosciences). Kit+ cells were cultured at 10^6/mL with Iscove modified Dulbecco medium (Invitrogen), 20% BIT 9500 (Stem Cell Technologies), and 100 ng/mL TPO (Peprotech). After 4 days at 37°C/5% CO_2, 300 ng/mL SDF-1 (Peprotech) or vehicle was added for 1 hour. Cells were washed in PB2, stained, and analyzed by imaging flow cytometry.[50]

Immunohistochemistry

Hindlimbs were fixed in 4% paraformaldehyde for 24 hours, decalcified in either 10% EDTA for 10 to 14 days or Richard Allen Decalcifying Solution (Thermo-Fisher) for 5 hours, and embedded in paraffin. Femoral sections (5 μm) underwent heat antigen retrieval (Dako), blocking with 5% goat serum (Vector Labs) and 5% bovine serum albumin (Gemini Bio-Products), and sequential antibody staining: 1:100 anti-panendothelial cell antigen (MECA32; Biolegend), 1:500 AlexaFluor647 goat anti-rat (Life Technologies), 1:300 anti-Gp1Bβ (Emfret), and 1:500 IRDye 800CW goat anti-rat (LI-COR). Images were acquired with an ORCA-R2 digital camera (Hamamatsu) with Nikon NIS-Elements software on an Eclipse 80i microscope (Nikon) with a ×20 objective. Total Gp1Bβ+ MKs and MKs physically associated with MECA32+ vessels were manually enumerated for 8 to 12 images per section (mean, 94 total MK/sample; range, 45-148). MECA32+ vessels were demarcated and vascular area/total marrow area was determined by NIS-Elements.

RNA in situ hybridization

Analysis of SDF-1 transcripts was performed on femoral sections, as previously described.[51,52] Darkfield and brightfield images were acquired with an ORCA-R2 digital camera (Hamamatsu) with Nikon NIS-Elements software on an Eclipse 80i microscope (Nikon) with a ×4 objective. For each darkfield image, signal threshold was set to capture single autoradiographic grains, and the grain area determined in a 100 μm × 1250 μm region at the endosteal boundary of diaphyseal marrow, as well as an immediately adjacent region in central marrow. The endosteal:central grain area ratio was obtained for each image. The images were processed and pseudocolored using Photoshop 6.0 (Adobe).

Gene expression analysis

RNA was isolated from flushed marrow and complementary DNA prepared, as previously described.[53] Quantitative polymerase chain reaction (qPCR) was performed with Taqman Gene Expression Assays (Life Technologies). CXCL12 (Mm00445553_m1) expression was normalized to 18S (Hs99999901_s1).

Results

Exogenous SDF-1 acutely increases MKs in the vascular niche and platelet output

Studies utilizing a murine model of constitutive plasma elevation of SDF-1 indicate that a sustained gradient of SDF-1 toward the vasculature results in increased MKs associated with marrow vasculature.[20] However, the extended timeframe of SDF-1 exposure, coupled with the capacity of the vascular niche to influence MK maturation[4,18,19] makes it difficult to determine direct SDF-1 effects on MK location. Given that the chemotactic response of MKs to SDF-1 in vitro occurs rapidly,[24,54] we asked if an exogenous gradient of SDF-1 toward the vasculature acutely regulates MK migration. A single 400 ng dose of SDF-1 was administered IV and the compartments of the MK lineage were analyzed 24 hours later. There was no change in the number of MKPs, defined functionally by colony assay, or MKs, determined by imaging flow cytometry, in the femurs of the mice treated with SDF-1 compared with vehicle controls (Figure 1A). Surprisingly, however, mice receiving SDF-1 had a 17% increase in platelet count (Figure 1A). This increase in circulating platelets was likely due to enhanced production, as platelets isolated from mice treated with SDF-1 had higher thiozole orange staining, which can label both RNA and dense granules, and indicates an increase in young, reticulated platelets[55,56] (Figure 1B). Further supporting an acute increase in thrombopoiesis, mice receiving SDF-1 had more exhausted MKs at 24 hours by imaging flow cytometry[10,11,50] (Figure 1C). Although there was no change in the total number of MKs (Figure 1A), as early as 1 hour after IV SDF-1 there was a dramatic shift in their location, with a >40% increase in the proportion of Gp1Bβ+ MKs associated with MECA32+ vasculature by immunohistochemistry (IHC) (Figure 1D-E).[57]

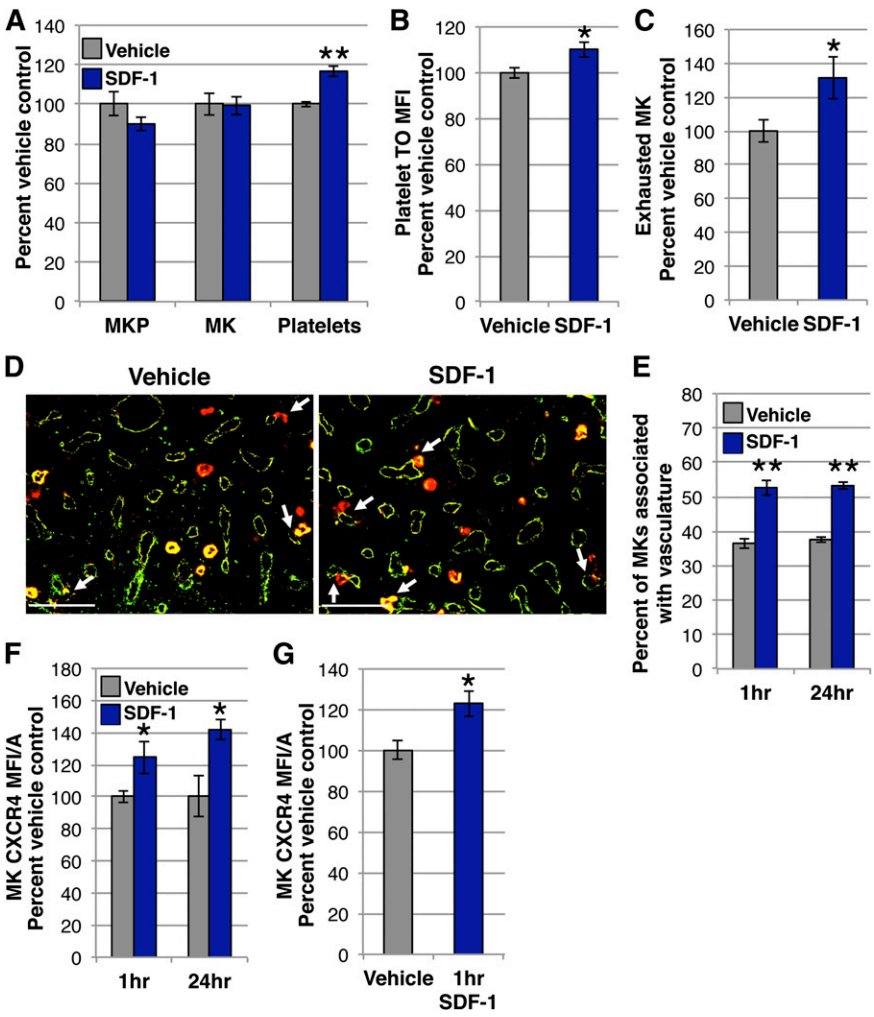

Figure 1. Vascular elevation of SDF-1 by IV administration acutely promotes the association of MKs with vasculature and thrombopoiesis. (A) MKP, MK, and platelet kinetics 24 hours after 400 ng IV SDF-1 (blue) or vehicle control (gray). SDF-1-treated mice have an acute increase in circulating platelets with no change in MK or MKP number in the marrow. MKP (colony assay) and MK (imaging flow cytometry) numbers are normalized to per femur values. Mean absolute numbers for vehicle controls: 16 905 MKP/femur, 45 939 MK/femur, 430 $\times$ 10^3 platelets/μL. (B) MFI of thiozole orange (TO) in platelets identified as $CD41^+Ter119$- by imaging flow cytometry 24 hours after IV SDF-1 or vehicle. Platelets from SDF-1–treated mice have increased TO staining. (C) The proportion of exhausted MKs was identified by imaging flow cytometry and presented as percent of vehicle control for each experiment. Mean proportion of exhausted MKs for vehicle controls: 0.14. (D) Representative images of femoral marrow immunohistochemistry (IHC) for Gp1Bβ (MKs, red) and MECA32 (vascular endothelium, green) 24 hours after IV treatment with vehicle (left panel) or SDF-1 (right panel). White arrows indicate examples of MKs physically associated with MECA32+ vessels. Some MKs express the pan-endothelial antigen recognized by MECA32.[57] Images were processed as described in the "Immunohistochemistry" section. (E) Quantification of Gp1Bβ+ MKs physically associated with MECA32+ vessels by manual counting of IHC 1 hour and 24 hours after IV SDF-1 (blue) or vehicle (gray). IV SDF-1 acutely increases MK association with the vasculature. (F) MFI/A of surface CXCR4 on primary MKs by imaging flow cytometry of flushed marrow samples prepared 1 hour and 24 hours after IV SDF-1 (blue) or vehicle (gray). (G) MFI/A of surface CXCR4 on in vitro–derived MKs 1 hour after SDF-1 treatment (blue) by imaging flow cytometry. SDF-1 treatment increases MK surface CXCR4 both in vivo (F) and in vitro (G). Error bars represent standard error of the mean of $\geq$3 independent experiments (n = 6-18 total mice per group). Statistical analyses comparing SDF-1 to vehicle controls were performed using a 2-tailed Student's *t* test. Bar represents 100 μm (D). $^*P < .04$; $^{**}P < .005$.

As changes in CXCR4 expression have been noted after SDF-1 stimulation in many cell types,[58-62] we investigated CXCR4 surface expression on MKs by imaging flow cytometry. MKs isolated 1 hour and 24 hours after IV SDF-1 demonstrated increased surface expression of the CXCR4 receptor (Figure 1F). In vitro–derived primary MKs displayed a similar increase in CXCR4 expression at 1 hour, suggesting this is a direct response of MKs to SDF-1 stimulation (Figure 1G). Taken together, these results indicate that acute elevation of vascular SDF-1 with IV administration rapidly enhances the MK-vasculature association, which leads to increased platelet production.

Stabilization of endogenous SDF-1 enhances MK-vasculature interactions and increases circulating platelets

Next, we sought to determine if the migration of MKs during steady-state megakaryopoiesis is regulated by a native, endogenous SDF-1 gradient. In vivo, SDF-1 contributes to chemotactic gradients in close proximity to its synthesis, as it binds many glycosaminoglycan extracellular matrix components upon secretion and can undergo rapid proteolysis.[63,64] To stabilize endogenously-produced SDF-1, we used Diprotin A, a small peptide that inhibits dipeptidyl peptidase 4 (DPP4), a soluble and cell-surface protease present in the bone marrow that truncates SDF-1 and abolishes its chemotactic activity.[65-68] There were no changes in the number of marrow MKPs or MKs by 24 hours after administration of Diprotin A; however, there was a 20% increase in circulating platelets (Figure 2A). Similar to the response of MKs to exogenous SDF-1 (Figure 1F), marrow MKs had increased surface CXCR4 1 hour after Diprotin A-mediated stabilization of SDF-1 (Figure 2B). Significantly, mice receiving Diprotin A also demonstrated a 30% increase in MKs associated with the vasculature by IHC (Figure 2C-D). These results mirror the MK shift toward the vascular niche and increased platelet production seen with the acute administration of IV SDF-1 (Figure 1), supporting the concept that SDF-1 regulates the maturational movement of MKs toward the vasculature during normal megakaryopoiesis.

Sublethal TBI induces temporal and spatial changes in marrow SDF-1

As SDF-1 contributes to MK localization to the thrombopoietic niche at steady state, we asked whether changes in marrow SDF-1 have consequences for the MK lineage. Given the importance of the location of SDF-1 production for its chemotactic function,[63] and the varied injury and recovery kinetics of different marrow cell populations after sublethal TBI,[40-43] we reasoned there might be changes in marrow SDF-1 gradients in this injury setting. To address this, we investigated the location of SDF-1 transcripts in the marrow of mice after sublethal 4 Gy TBI by radioactive in situ hybridization (Figure 3A). As expected, there was an overall increase in SDF-1 message in the marrow following TBI,[39,46] which was confirmed by qPCR (Figure 3B). There were, however, no changes in plasma

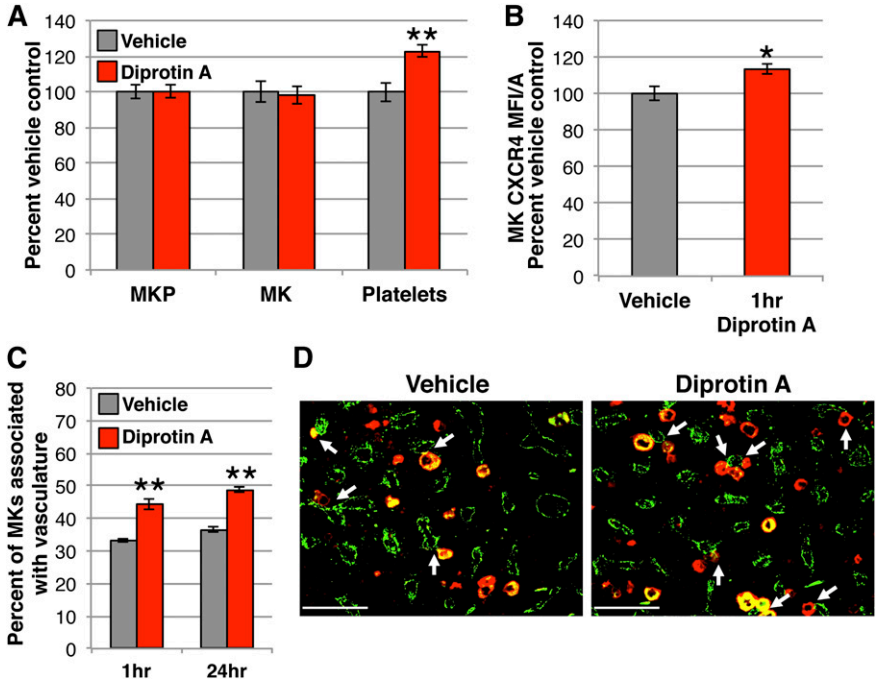

Figure 2. Native SDF-1 enhances MKs in the vascular niche and increases circulating platelets. (A) MKP, MK, and platelet kinetics 24 hours after 1.7 mg (5 μmol) intraperitoneal Diprotin A (red) or vehicle control (gray). Stabilization of SDF-1 with Diprotin A acutely increases circulating platelets with no change in MK or MKP number in the marrow. MKP (colony assay) and MK (imaging flow cytometry) numbers are normalized to per femur values and all compartments expressed as percent of vehicle control. Mean absolute numbers for vehicle controls: 11 593 MKP/femur, 49 856 MK/femur, 436 × 10^3 platelets/μL. (B) MFI/A of surface CXCR4 on primary MKs by imaging flow cytometry of flushed marrow samples prepared 1 hour after treatment with Diprotin A (red) or vehicle control (gray). (C) Quantification of Gp1Bβ+ MKs physically associated with MECA32+ vessels by IHC 1 hour and 24 hours following treatment with Diprotin A (red) or vehicle (gray). Diprotin A-mediated stabilization of SDF-1 acutely increases MK association with the vasculature. (D) Representative images of femoral marrow IHC for Gp1Bβ (MKs, red) and MECA32 (vascular endothelium, green) 24 hours after administration of vehicle (left panel) or Diprotin A (right panel). White arrows indicate examples of MKs physically associated with MECA32+ vessels. Images were processed as described in the "Immunohistochemistry" section. Error bars represent standard error of the mean of ≥3 independent experiments (n = 7-8 total mice per group). Statistical analyses comparing Diprotin A to vehicle controls were performed using a 2-tailed Student's *t* test. Bar represents 100 μm (D). *$P < .02$; **$P < .003$.

SDF-1 protein levels in the first 4 days after injury (supplemental Figure 1 available on the *Blood* Web site). Changes in marrow distribution were quantified by comparing SDF-1 transcript levels within the endosteal region in the diaphyseal marrow to the levels in an adjacent region within the central marrow (Figure 3C). Interestingly, we detected the development of an SDF-1 gradient toward the endosteum at day 2 that was no longer present at day 3 (Figure 3C).

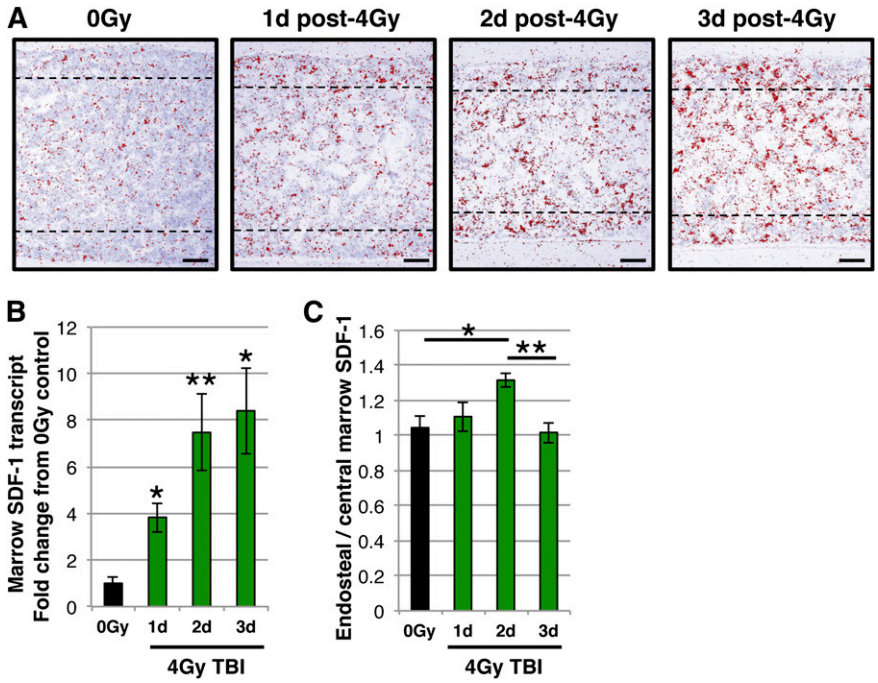

Figure 3. Temporal and spatial changes in marrow SDF-1 following sublethal radiation. (A) Representative images of radioactive in situ hybridization with SDF-1 antisense probe (red pseudocolor indicates SDF-1 transcripts) on femoral marrow sections from (left to right panels): unirradiated (0 Gy), and days 1, 2, and 3 post-4 Gy TBI. Dotted lines delineate the endosteal region. Images were acquired and processed as described in the "RNA in situ hybridization." (B) Expression of SDF-1 transcripts by qPCR in flushed marrow cells from unirradiated mice (black) and days 1, 2, and 3 post-4 Gy TBI (green). SDF-1 transcripts increase in the marrow following TBI. (C) Ratio of SDF-1 transcript area in the endosteal region (between 0-100 μm from the endosteal surface within the diaphysis) compared to an immediately adjacent region of the same size (between 100-200 μm from the endosteal surface) for each biologic replicate of unirradiated mice (black), and days 1, 2, and 3 post-4 Gy TBI (green). An endosteal gradient of SDF-1 transcript is apparent at day 2, but is lost at day 3. Error bars represent standard error of the mean of ≥3 independent experiments (n = 3-7 total mice per group). Statistical analyses either comparing irradiated samples to unirradiated control (B) or indicated samples (C) were performed using a 2-tailed Student's *t* test. Bar represents 100 μm (A). *$P < .02$; **$P < .007$.

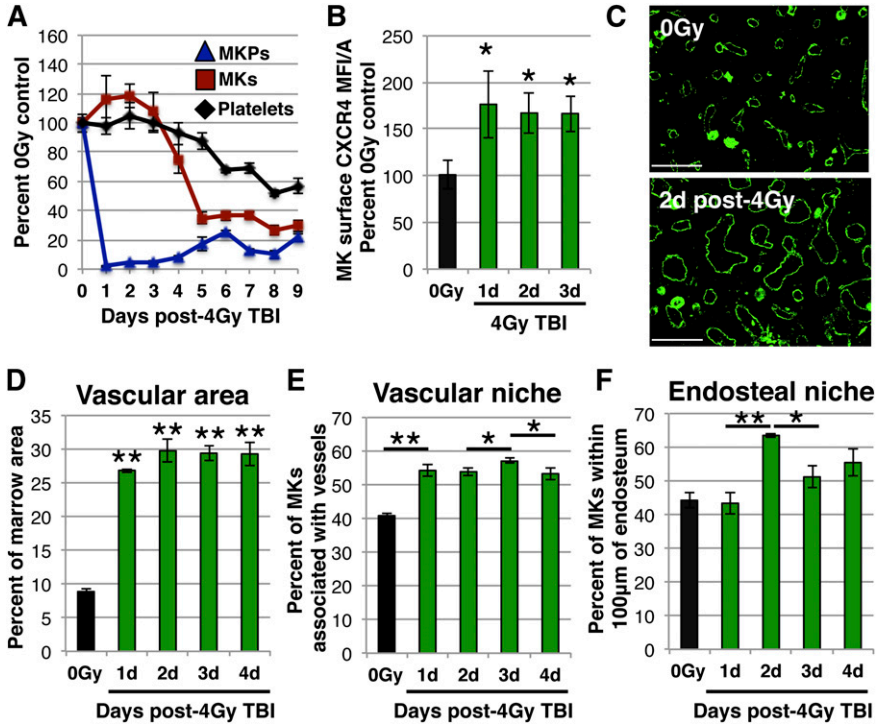

Figure 4. Altered niche occupancy of radioresistant MKs following sublethal radiation. (A) MK lineage injury kinetics following 4 Gy TBI. Circulating platelets (black) and marrow MKs (red) remain at steady-state levels for 3 days (one-way analysis of variance, $P = .45$), while upstream MKPs (blue) are rapidly lost. MKP (colony assay) and MK (imaging flow cytometry) numbers are normalized to per femur values and all compartments expressed as percent of unirradiated control. Mean absolute numbers for 0 Gy controls: 13 550 MKP/femur, 56 022 MK/femur, 484 $\times$ 10^3 platelets/μL. (B) MFI/A of surface CXCR4 on primary MKs by imaging flow cytometry of flushed marrow samples prepared from unirradiated controls (black) or days 1 to 3 post-4 Gy TBI (green). MKs from irradiated mice display increased surface CXCR4 expression. (C) Representative images of femoral IHC for MECA32 (vasculature, green) with hindlimbs isolated from unirradiated mice (top panel) or day 2 post-4 Gy TBI (bottom panel). The marrow vasculature dilates after TBI. (D) Quantification of vascular area within MECA32+ marrow vessels by IHC. Vascular dilation occurs by day 1 after injury and remains constant from days 1 to 4 post-4 Gy TBI. (E) Quantification of Gp1Bβ+ MKs physically associated with MECA32+ vessels by femoral IHC prepared from unirradiated control mice (black) or days 1 to 4 post-4 Gy TBI (green). MK association with vasculature changes dynamically following radiation, increasing between days 0 and 1 and between days 2 and 3, but decreasing between days 3 and 4. (F) Quantification of Gp1Bβ+ MKs in the endosteal niche (within 100 μm of the endosteal surface within diaphysis) by IHC in unirradiated control mice (black) and days 1 to 4 post-4 Gy TBI (green). MKs increase in the endosteal niche between days 1 and 2, and decrease between days 2 and 3. Image processing and analysis is described in the "Immunohistochemistry" section. The vascular niche and endosteal niche measurements were not made in a mutually exclusive manner and there may be overlap in occupancy between these niches. Error bars represent standard error of the mean of $\geq$3 independent experiments (n = 3-12 total mice per group). Statistical analyses either comparing irradiated samples to unirradiated control (B and D) or indicated samples (E and F) were performed using a 2-tailed Student's *t* test. Bar represents 100 μm (C). *$P < .04$; **$P < .001$.

Radioresistant MKs display altered marrow niche occupancy after sublethal TBI

To determine whether MKs respond to the observed shifts in SDF-1 expression following 4 Gy TBI, we first characterized the injury kinetics of the MK lineage (Figure 4A). Platelets remained at steady-state levels for 4 days, followed by the development of thrombocytopenia, with a nadir in platelet count at day 8 following TBI (Figure 4A). MKs persisted during the first 3 days postinjury (Figure 4A), despite the loss of >85% of nucleated marrow cells (data not shown). Importantly, these radioresistant MKs had increased surface expression of CXCR4, indicating they retained the ability to respond to SDF-1 (Figure 4B; supplemental Figure 1). Megakaryocytopenia and thrombocytopenia eventually develop as a consequence of the rapid, near complete loss of the upstream MKP compartment (Figure 4A).

Since MKs interact with sinusoidal endothelium, we also examined the effects of 4 Gy TBI on marrow vasculature by IHC. Most notable was a marked vascular dilation at day 1 post-TBI, with a 200% increase in the marrow area occupied by vasculature that persisted for at least 4 days following the injury (Figure 4C-D; supplemental Figure 2). Accompanying the early, rapid vascular dilation was a 30% increase in the MKs associated with sinusoids by IHC at day 1 (Figure 4E). The temporal overlap between the vascular changes and the shift in MK-vasculature association suggests that this initial change in MK niche occupancy is likely secondary to vascular dilation. However, within the subsequent timeframe in which vascular dilation remains constant, there were small, but significant changes in MKs in the vascular niche, suggesting additional factors may influence this altered localization (Figure 4E).

Given the development of an SDF-1 gradient toward the endosteum following TBI (Figure 3A,C), we also quantified MK distribution in the endosteal niche, defined as within 100 μm of the diaphyseal endosteum[69] (Figure 4F). Strikingly, there was a 45% increase in radioresistant MKs in the endosteal niche between days 1 and 2 post-TBI (Figure 4F). MKs rapidly decreased in the endosteal niche by day 3 postinjury (Figure 4F), coincident with the diminished SDF-1 gradient (Figure 3A,C). Taken together, these results spatially and temporally implicate alterations in marrow SDF-1 after TBI in MK niche occupancy changes.

Stabilization of altered SDF-1 gradients post-TBI functionally regulate MK location and platelet production

We hypothesized that changes in the spatial localization of MKs between days 2 and 3 post-TBI were regulated by shifts in marrow SDF-1 production. In light of the importance of MK-vasculature association for efficient platelet production,[21] we reasoned that

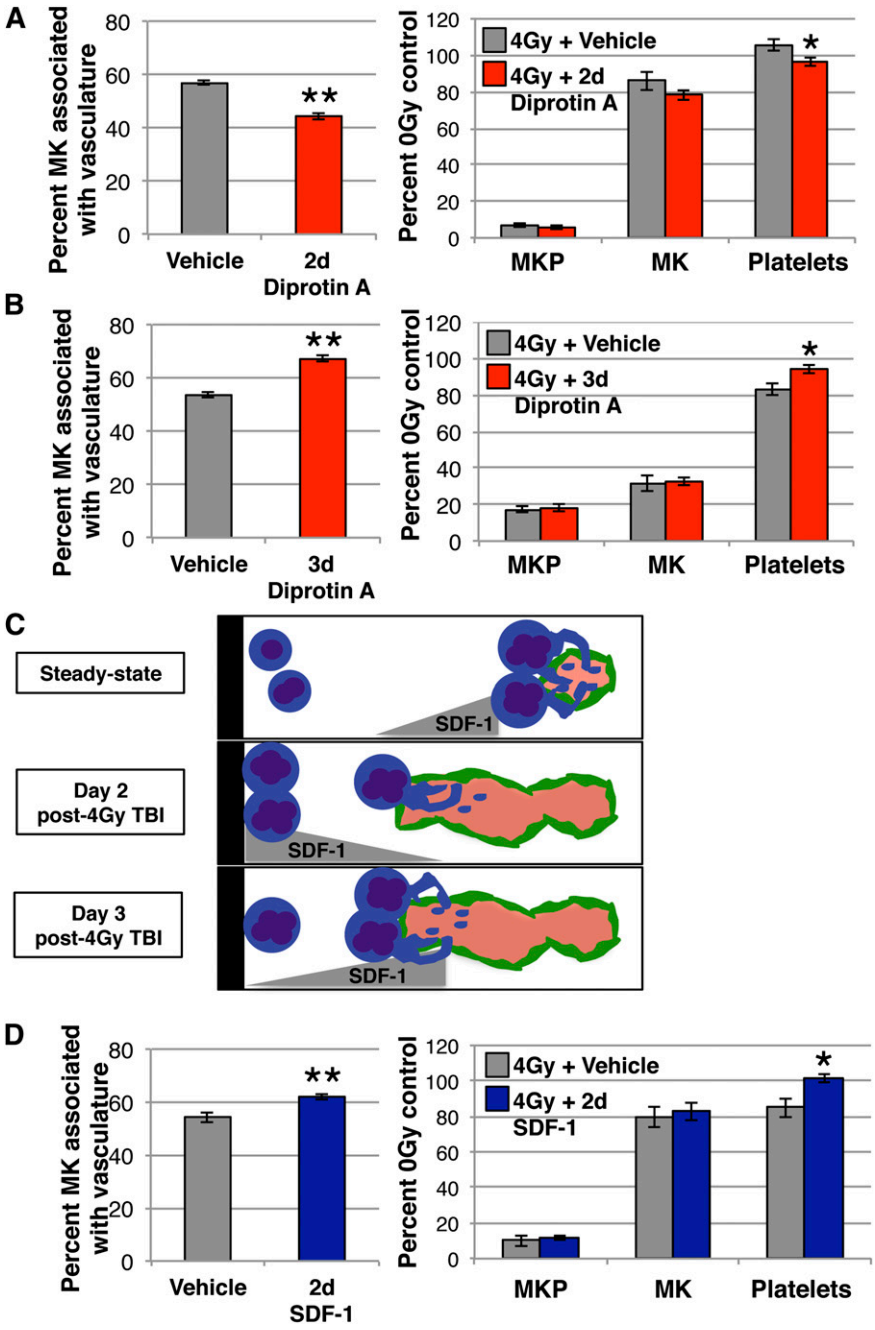

Figure 5. Changes in SDF-1 regulate MK spatial location and platelet production following 4 Gy TBI. (A) Analysis of MK lineage kinetics (right panel) and Gp1Bβ+ MKs physically associated with MECA32+ vasculature (left panel) 24 hours after treatment with Diprotin A (red) or vehicle (gray) at day 2 post-4 Gy TBI. Diprotin A-mediated stabilization of SDF-1 at day 2 following TBI decreases platelets and MKs in the vascular niche. MKP (colony assay) and MK (imaging flow cytometry) numbers are normalized to per femur values and all compartments are expressed as percent of unirradiated control. Mean absolute numbers for 0 Gy controls: 12 420 MKP/femur, 53 946 MK/femur, 470 × 10^3 platelets/μL. (B) Analysis of MK lineage kinetics (right panel) and Gp1Bβ+ MKs physically associated with MECA32+ vasculature (left panel) 24 hours after treatment with Diprotin A (red) or vehicle (gray) at day 3 post-4 Gy TBI. Diprotin A-mediated stabilization of SDF-1 at day 3 increases platelets and MKs in the vascular niche. MKP (colony assay) and MK (imaging flow cytometry) numbers are normalized to per femur values and all compartments expressed as percent of unirradiated control. Mean absolute numbers for 0 Gy controls: 13 272 MKP/femur, 52 414 MK/femur, 491 × 10^3 platelets/μL. (C) Model depicting the regulation of MK niche occupancy in the marrow by SDF-1 at steady state (top panel) and days 2 (middle panel) and 3 (bottom panel) after 4 Gy TBI. At a steady state, Diprotin A-mediated stabilization of SDF-1 increases MKs in the vascular niche. At day 2 following TBI, when our studies reveal a gradient of SDF-1 toward the endosteum, stabilization of SDF-1 decreases both MK association with vasculature and the number of circulating platelets. In contrast, at day 3 post-TBI, when the endosteal SDF-1 gradient is lost, stabilization of SDF-1 resembles the steady-state condition with increased MKs in the vascular niche. (D) Analysis of MK lineage kinetics (right panel) and Gp1Bβ+ MKs physically associated with MECA32+ vasculature (left panel) 24 hours after IV SDF-1 administration (blue) or vehicle (gray) at day 2 post-4 Gy TBI. At this time point, elevation of vascular SDF-1 with IV administration counteracts the endogenous endosteal SDF-1 gradient and leads to enhanced MK-vasculature association and increased circulating platelets. Mean absolute numbers for 0 Gy controls: 10 996 MKP/femur, 52 615 MK/femur, 459 × 10^3 platelets/μL. Error bars represent standard error of the mean of ≥3 independent experiments (n = 5-9 total mice per group). Statistical analyses comparing treated mice to vehicle controls were performed using a 2-tailed Student's *t* test. *$P \leq .04$; **$P < .006$.

alterations in MK niche occupancy would affect platelet production. To address this, we stabilized native SDF-1 with Diprotin A at day 2 post-TBI, when SDF-1 production is increased near the endosteum, and found a 20% decrease in MKs in the vascular niche (Figure 5A, left panel) and a small, but significant decrease in circulating platelets 24 hours later (Figure 5A, right panel). However, stabilization of SDF-1 at day 3 post-TBI, when there is no longer an endosteal SDF-1 gradient, has opposing effects, with significant increases both in MK-vasculature association (Figure 5B, left panel) and in platelet count (Figure 5B, right panel). These data support the concept that changes in the location of SDF-1 production at days 2 and 3 after TBI contribute to altered MK location in the marrow (Figure 5C). Additionally, these results demonstrate that the spatial distribution of MKs has functional consequences, as MKs leaving the vascular niche decreases circulating platelets while enhanced MK-vasculature association increases platelet numbers.

Having shown that a transient increase in endosteal SDF-1 production directs MKs away from the vascular niche and negatively affects platelet production, we asked whether we could manipulate MK location and influence platelet output by altering SDF-1 gradients. To this end, we elevated vascular SDF-1 with acute IV administration at day 2 postinjury, when there is a native increase in endosteal SDF-1. Whereas Diprotin A-mediated stabilization of endogenous-produced SDF-1 at day 2 decreases both MK association with the vasculature and platelet production 24 hours later (Figure 5A), IV SDF-1 had opposing effects, increasing MKs in the vascular niche (Figure 5D, left panel) as well as circulating platelets (Figure 5D, right panel). Taken together, these data highlight

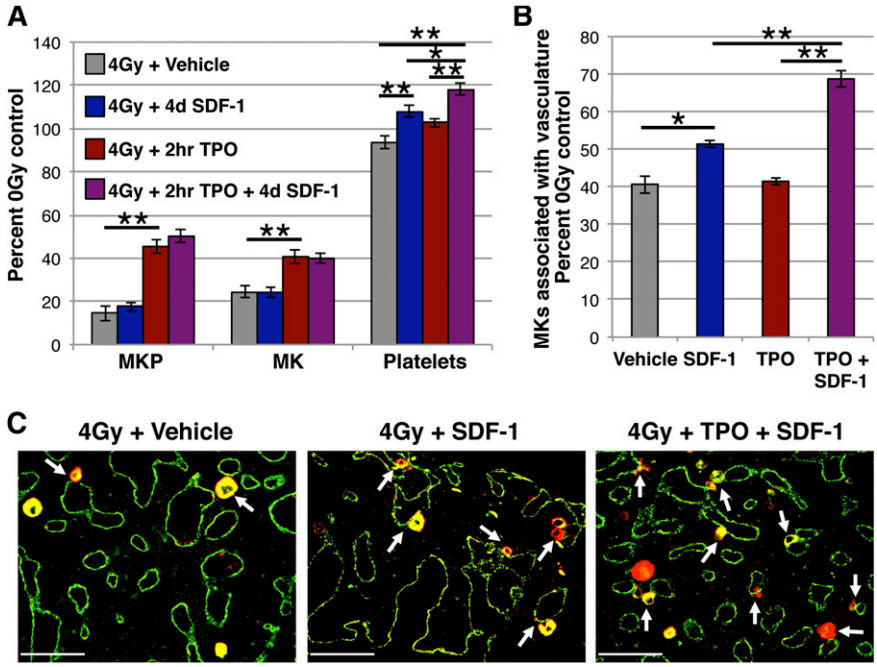

Figure 6. Acute administration of IV SDF-1 improves radiation-induced thrombocytopenia and is an additive with earlier TPO administration. (A) MK lineage kinetics at day 5 post-4 Gy TBI in mice treated with IV SDF-1 at day 4 (blue), 0.3 μg IP TPO (red) at 2 hours, both 2-hour TPO and day 4 SDF-1 (purple), or vehicle control (gray). IV SDF-1 increases platelet count following radiation injury. TPO administration at 2 hours post-TBI increases MK and MKP numbers, and IV SDF-1 at day 4 following initial TPO treatment results in an additive improvement in circulating platelets. MKP (colony assay) and MK (imaging flow cytometry) numbers are normalized to per femur values and all compartments expressed as a percentage of unirradiated control. Mean absolute numbers for 0 Gy controls: 10 939 MKP/femur, 50 595 MK/femur, 473 × 10^3 platelets/μL. (B) Quantification of Gp1Bβ+ MKs in the vascular niche (physically associated with MECA32+ vessels) by femoral IHC prepared on day 5 post-4 Gy from irradiated vehicle control mice (gray), or mice treated with IV SDF-1 at day 4 (blue), 0.3 μg IP TPO (red) at 2 hours, or both 2-hour TPO and day 4 SDF-1 (purple). Percentage of MKs associated with vasculature (IHC) are normalized to per femur values (imaging flow cytometry). Mean 20 104 MK/femur associated with vasculature for 0 Gy controls. Sequential TPO and SDF-1 administration increases MKs in the vascular niche above either treatment alone. (C) Representative images of femoral marrow IHC for Gp1Bβ (MKs, red) and MECA32 (vascular endothelium, green) at day 5 post-4 Gy with hindlimbs isolated from vehicle controls (left panel), mice receiving IV SDF-1 at day 4 (middle panel), and mice receiving 2-hour TPO followed by day 4 SDF-1 (right panel) as described above. White arrows indicate examples of MKs physically associated with MECA32+ vessels. Images were acquired and processed as described in the "Immunohistochemistry" section. Error bars represent standard error of the mean of ≥3 independent experiments (n = 3-11 total mice per group). Statistical analyses comparing indicated platelet samples in panel A were performed by one-way analysis of variance with Tukey's multiple comparisons test, and all other indicated comparisons were performed by a 2-tailed Student's *t* test. Bar represents 100 μm (C). *$P < .05$; **$P < .006$.

the direct effects of rapidly changing SDF-1 gradients on MK spatial localization and thrombopoiesis.

Administration of SDF-1 improves radiation-induced thrombocytopenia in a manner additive with prior TPO administration

Our studies indicate that appropriately timed IV administration of SDF-1 can acutely increase platelet output. To test whether this strategy could be used to improve radiation-induced thrombocytopenia, we administered SDF-1 on day 4 after 4 Gy TBI, when thrombocytopenia begins to develop (Figure 4A), and our localization studies indicate a small decrease of MKs within the vascular niche (Figure 4E). With no change in MKP or MK number 24 hours following IV SDF-1 (day 5 post-TBI), there were increases in both platelet count and MKs associated with the vasculature (Figure 6A-C). However, these effects were less robust than those achieved with the same dose of SDF-1 in uninjured mice (Figure 1A). We hypothesized this was a consequence of fewer MKs present in the marrow to move to the vascular niche at this time point postinjury, and the SDF-1-mediated platelet increase may therefore depend on MK availability.

Treatment with the cytokine TPO increases the number of MKs in the marrow and has been shown to improve MK lineage recovery when administered after sublethal TBI in mice.[12,13,70] In our model, administration of TPO 2 hours following 4 Gy TBI resulted in a >200% expansion of MKPs, a 65% increase in MKs, and a small, but not statistically significant increase in platelet count (Figure 6A). Mice receiving TPO at 2 hours followed by SDF-1 at day 4 had an additive increase in circulating platelets compared with either treatment alone (Figure 6A), and a corresponding 70% increase in MKs associated with the vasculature (Figure 6B-C). These data suggest that the platelet increase accompanying SDF-1-mediated localization of MKs to the vascular niche is dependent, at least in part, on the number of MKs available to relocate. Additionally, our results indicate that a sequential combination of TPO, which increases MK number, followed by SDF-1, which enhances MK localization in the thrombopoietic niche and platelet output, may be a potent strategy to acutely improve thrombocytopenia in the setting of radiation injury.

Discussion

The working paradigm of megakaryopoiesis and thrombopoiesis has been primarily cytokine-driven, based on the potent ability of TPO to increase MK numbers and accelerate MK maturation, thereby indirectly enhancing platelet production.[13,14,71] Elegant studies by Avecilla et al[20] identified the chemokine SDF-1 as a TPO-independent promoter of thrombopoiesis. However, the extended timeframe of vascular SDF-1 elevation in these studies complicates the evaluation

of in vivo effects on MK chemotaxis vs a direct role for SDF-1 and/or endothelium in MK lineage maturation.[20] Furthermore, there are conflicting in vitro reports concerning a role for SDF-1 in MKP proliferation and MK maturation.[22,72,73] Here, we directly addressed the acute effects of exogenous SDF-1 using a single IV administration, which only circulates for minutes to hours.[64] With a quantitative IHC approach, we found MKs redistribute to the vasculature within 1 hour of SDF-1 administration (Figure 1E). Importantly, this rapid SDF-1-mediated association of MKs with the vasculature is also accompanied by an increase in circulating platelets apparent at 24 hours (Figure 1). In vitro treatment of MKs with SDF-1 does not yield an increase in platelets (data not shown), suggesting that SDF-1 directly contributes to MK movement to the vasculature, whereas the increase in thrombopoiesis is likely due to instructive cues from the vascular niche.[4,18,19,74]

To our knowledge, these studies are the first to demonstrate that natively produced SDF-1 directs MK migration to the vascular niche (Figure 2). For the stabilization of endogenous SDF-1, we used tripeptide Diprotin A to inhibit DPP4, a peptidase that inactivates SDF-1.[66,75] This strategy has been used to stabilize SDF-1 in several contexts, including the homing and engraftment of hematopoietic stem cells and the recruitment of marrow-derived progenitors to sites of cardiac ischemia for myocardial regeneration.[68,76-78] DPP4 was recently shown to truncate several cytokines, including IL-6, and is predicted to truncate TPO.[79] While we cannot exclude effects of stabilization of these cytokines by Diprotin A, the short timeframe of our experiments coupled with the lack of change in the number or ploidy distribution of MKs (Figure 1A; supplemental Figure 3) supports SDF-1 as the mediator of spatial changes following Diprotin A treatment. Longer term inhibition of DPP4 may uncover cytokine-driven effects on the MK lineage as $Dpp4^{-/-}$ mice have increased numbers of MKPs and MKs.[80]

CXCR4 can be internalized after SDF-1 stimulation, and either recycled to the membrane or degraded.[81] Unexpectedly, we found that acute stimulation with SDF-1 resulted in a small, but significant increase in CXCR4 on the surface of MKs both in vitro and in vivo, as well as following stabilization of SDF-1 in vivo (Figure 1F-G and 2B). It has been reported that SDF-1 induces CXCR4 promoter activity[59] and activated nuclear factor κB, which is downstream of SDF-1/CXCR4 signaling in MKs,[26] can also induce CXCR4 transcription.[58] In addition, SDF-1/CXCR4 signaling in MKs induces vascular endothelial growth factor production,[26] which can increase MK surface CXCR4.[34] Moreover, the observed increase in surface CXCR4 could result from the translocation of intracellular stores of CXCR4 to the cell surface, which has been reported in hematopoietic progenitor cells.[82] Following radiation injury, the upregulation of MK surface CXCR4 could also be due to microenvironmental hypoxia through HIF-1α[83] (Figure 4B).

Our studies reveal spatial fluctuations in SDF-1 transcript production in the marrow following sublethal TBI that dynamically regulate MK location. Despite loss of the vast majority of nucleated marrow cells following TBI, we confirmed a global increase in marrow SDF-1 transcripts (Figure 3B). These data are in-line with the induction of SDF-1 expression after radiation injury in rodents and in humans, through HIF1α-dependent and HIF1α-independent pathways.[39,46,84-86] More relevant for chemotactic function, we identified a transient elevation of SDF-1 transcripts near the endosteum at day 2 following injury that directs MKs away from the vascular niche (Figures 3C and 5A). Evidence pointing to a cell population that may contribute to altered SDF-1 distribution comes from the work of Dominici et al,[39] Olson et al,[47] and Caselli et al[87] who described an expansion of osteoblasts arising from a subset of radioresistant mesenchymal cells at the endosteal surface concomitant with MK relocation following lethal TBI. Mesenchymal stromal and progenitor cells are some of the highest producers of SDF-1 in the marrow at steady state[29,31,32] and are relatively radioresistant,[88] suggesting these populations may participate in marrow microenvironmental changes following TBI. Further investigation to specifically identify the SDF-1–producing cells pertinent for MKs at steady state and postinjury may lead to new strategies to influence platelet production by controlling MK niche occupancy. Additionally, while this work focused on the thrombopoietic vascular niche because of its functionality for MKs, it remains an open question whether alterations in microenvironmental SDF-1 following sublethal radiation injury affect the location or function of other hematopoietic cells. This may be particularly relevant for hematopoietic stem and progenitor cells, which are regulated by SDF-1[29,31,32,89] and have been found in close proximity to diverse marrow microvessels,[90] including preferentially arteriolar vasculature in the endosteal region.[91]

Significantly, our studies establish that acute manipulation of SDF-1 has functional consequences for MK location and platelet production. We tested the validity of this concept in a model of radiation-induced thrombocytopenia. While SDF-1 increases MK association with the vasculature and improves thrombocytopenia, there is an additive increase in circulating platelets if the number of marrow MKs is increased with TPO administration prior to SDF-1 treatment. These data suggest a potential sequential therapeutic approach combining an agent that first increases the number of MKs in the marrow followed by an agent that shifts their location to the vascular niche to promote platelet production. Additionally, the ability to acutely elevate circulating platelets within 24 hours may have therapeutic relevance in certain scenarios as the current clinically available Mpl agonists require 5 days to begin elevating platelet counts.[92,93]

Taken together, our data indicate that SDF-1 acutely regulates MK location in the bone marrow. At steady state, SDF-1 directs MKs to the vascular niche, resulting in thrombopoiesis. Following radiation injury, dynamic changes in microenvironmental SDF-1 alter the location of radioresistant MKs in the marrow. Ultimately, we demonstrate that rational manipulation of SDF-1 can acutely improve thrombocytopenia by enhancing MK migration to the thrombopoiesis-promoting vascular niche.

Acknowledgments

The authors thank Jennifer McLaughlin for assistance with tissue sectioning, and gratefully acknowledge the technical support of Dr Tim Bushnell and Flow Cytometry Core Facility at the University of Rochester Medical Center.

This work was supported by funding from The National Institutes of Health (NIH), National Institute of Allergy and Infectious Diseases (R01AI080401 and U19AI091036) (J.P.), NIH, National Institute of Diabetes and Digestive and Kidney Diseases (F30DK100164) (L.M.N.), and the Michael Napoleone Foundation. L.M.N. is a trainee in the Medical Scientist Training Program funded by the NIH, National Institute of General Medical Sciences (T32GM07356).

Authorship

Contribution: L.M.N. designed and performed experiments, analyzed data, and wrote the manuscript; K.H.F. and P.D.K. designed and performed experiments; K.E.M. designed experiments and

analyzed data; and J.P. designed experiments, analyzed data, and wrote the manuscript.

Conflict-of-interest disclosure: The authors declare no competing financial interests.

Correspondence: James Palis, Department of Pediatrics, University of Rochester Medical Center, Center for Pediatric Biomedical Research, 601 Elmwood Ave, Box 703, Rochester, NY 14642; e-mail: james_palis@urmc.rochester.edu.

References

1. Metcalf D, MacDonald HR, Odartchenko N, Sordat B. Growth of mouse megakaryocyte colonies in vitro. *Proc Natl Acad Sci USA.* 1975; 72(5):1744-1748.
2. Williams N, Jackson H. Regulation of proliferation of murine megakaryocyte progenitor cells by cell cycle. *Blood.* 1978;52(1):163-170.
3. Shackney SE, Ford SS, Wittig AB. Kinetic-microarchitectural correlations in the bone marrow of the mouse. *Cell Tissue Kinet.* 1975;8(6): 505-516.
4. Mostafa SS, Miller WM, Papoutsakis ET. Oxygen tension influences the differentiation, maturation and apoptosis of human megakaryocytes. *Br J Haematol.* 2000;111(3):879-889.
5. Sabri S, Jandrot-Perrus M, Bertoglio J, et al. Differential regulation of actin stress fiber assembly and proplatelet formation by alpha2beta1 integrin and GPVI in human megakaryocytes. *Blood.* 2004;104(10): 3117-3125.
6. Pallotta I, Lovett M, Rice W, Kaplan DL, Balduini A. Bone marrow osteoblastic niche: a new model to study physiological regulation of megakaryopoiesis. *PLoS ONE.* 2009;4(12):e8359.
7. Odell TT Jr, Jackson CW. Polyploidy and maturation of rat megakaryocytes. *Blood.* 1968; 32(1):102-110.
8. Italiano JE Jr, Lecine P, Shivdasani RA, Hartwig JH. Blood platelets are assembled principally at the ends of proplatelet processes produced by differentiated megakaryocytes. *J Cell Biol.* 1999; 147(6):1299-1312.
9. Junt T, Schulze H, Chen Z, et al. Dynamic visualization of thrombopoiesis within bone marrow. *Science.* 2007;317(5845):1767-1770.
10. Behnke O. An electron microscope study of the rat megacaryocyte. II. Some aspects of platelet release and microtubules. *J Ultrastruct Res.* 1969; 26(1):111-129.
11. Radley JM, Haller CJ. Fate of senescent megakaryocytes in the bone marrow. *Br J Haematol.* 1983;53(2):277-287.
12. de Sauvage FJ, Hass PE, Spencer SD, et al. Stimulation of megakaryocytopoiesis and thrombopoiesis by the c-Mpl ligand. *Nature.* 1994; 369(6481):533-538.
13. Kaushansky K, Lok S, Holly RD, et al. Promotion of megakaryocyte progenitor expansion and differentiation by the c-Mpl ligand thrombopoietin. *Nature.* 1994;369(6481):568-571.
14. Banu N, Wang JF, Deng B, Groopman JE, Avraham H. Modulation of megakaryocytopoiesis by thrombopoietin: the c-Mpl ligand. *Blood.* 1995; 86(4):1331-1338.
15. Lichtman MA, Chamberlain JK, Simon W, Santillo PA. Parasinusoidal location of megakaryocytes in marrow: a determinant of platelet release. *Am J Hematol.* 1978;4(4):303-312.
16. Tavassoli M, Aoki M. Localization of megakaryocytes in the bone marrow. *Blood Cells.* 1989;15(1):3-14.
17. Rafii S, Shapiro F, Rimarachin J, et al. Isolation and characterization of human bone marrow microvascular endothelial cells: hematopoietic progenitor cell adhesion. *Blood.* 1994; 84(1):10-19.
18. Yang H, Miller WM, Papoutsakis ET. Higher pH promotes megakaryocytic maturation and apoptosis. *Stem Cells.* 2002;20(4):320-328.
19. Larson MK, Watson SP. Regulation of proplatelet formation and platelet release by integrin alpha IIb beta3. *Blood.* 2006;108(5):1509-1514.
20. Avecilla ST, Hattori K, Heissig B, et al. Chemokine-mediated interaction of hematopoietic progenitors with the bone marrow vascular niche is required for thrombopoiesis. *Nat Med.* 2004; 10(1):64-71.
21. Kopp H-G, Avecilla ST, Hooper AT, et al. Tie2 activation contributes to hemangiogenic regeneration after myelosuppression. *Blood.* 2005;106(2):505-513.
22. Wang JF, Liu ZY, Groopman JE. The alpha-chemokine receptor CXCR4 is expressed on the megakaryocytic lineage from progenitor to platelets and modulates migration and adhesion. *Blood.* 1998;92(3):756-764.
23. Rivière C, Subra F, Cohen-Solal K, et al. Phenotypic and functional evidence for the expression of CXCR4 receptor during megakaryocytopoiesis. *Blood.* 1999;93(5): 1511-1523.
24. Hamada T, Möhle R, Hesselgesser J, et al. Transendothelial migration of megakaryocytes in response to stromal cell-derived factor 1 (SDF-1) enhances platelet formation. *J Exp Med.* 1998; 188(3):539-548.
25. Dhanjal TS, Pendaries C, Ross EA, et al. A novel role for PECAM-1 in megakaryocytokinesis and recovery of platelet counts in thrombocytopenic mice. *Blood.* 2007;109(10):4237-4244.
26. Majka M, Ratajczak J, Kowalska MA, Ratajczak MZ. Binding of stromal derived factor-1alpha (SDF-1alpha) to CXCR4 chemokine receptor in normal human megakaryoblasts but not in platelets induces phosphorylation of mitogen-activated protein kinase p42/44 (MAPK), ELK-1 transcription factor and serine/threonine kinase AKT. *Eur J Haematol.* 2000;64(3):164-172.
27. Lane WJ, Dias S, Hattori K, et al. Stromal-derived factor 1-induced megakaryocyte migration and platelet production is dependent on matrix metalloproteinases. *Blood.* 2000;96(13): 4152-4159.
28. Sipkins DA, Wei X, Wu JW, et al. In vivo imaging of specialized bone marrow endothelial microdomains for tumour engraftment. *Nature.* 2005;435(7044):969-973.
29. Sugiyama T, Kohara H, Noda M, Nagasawa T. Maintenance of the hematopoietic stem cell pool by CXCL12-CXCR4 chemokine signaling in bone marrow stromal cell niches. *Immunity.* 2006;25(6): 977-988.
30. Méndez-Ferrer S, Michurina TV, Ferraro F, et al. Mesenchymal and haematopoietic stem cells form a unique bone marrow niche. *Nature.* 2010; 466(7308):829-834.
31. Ding L, Morrison SJ. Haematopoietic stem cells and early lymphoid progenitors occupy distinct bone marrow niches. *Nature.* 2013;495(7440): 231-235.
32. Greenbaum A, Hsu Y-MS, Day RB, et al. CXCL12 in early mesenchymal progenitors is required for haematopoietic stem-cell maintenance. *Nature.* 2013;495(7440):227-230.
33. Perez LE, Alpdogan O, Shieh J-H, et al. Increased plasma levels of stromal-derived factor-1 (SDF-1/CXCL12) enhance human thrombopoiesis and mobilize human colony-forming cells (CFC) in NOD/SCID mice. *Exp Hematol.* 2004;32(3):300-307.
34. Pitchford SC, Lodie T, Rankin SM. VEGFR1 stimulates a CXCR4-dependent translocation of megakaryocytes to the vascular niche, enhancing platelet production in mice. *Blood.* 2012;120(14): 2787-2795.
35. Dainiak N. Hematologic consequences of exposure to ionizing radiation. *Exp Hematol.* 2002;30(6):513-528.
36. Ebbe S, Stohlman F Jr. Stimulation of thrombocytopoiesis in irradiated mice. *Blood.* 1970;35(6):783-792.
37. Odell TT Jr, Jackson CW, Friday TJ. Effects of radiation on the thrombocytopoietic system of mice. *Radiat Res.* 1971;48(1):107-115.
38. Tanum G. The megakaryocyte DNA content and platelet formation after the sublethal whole body irradiation of rats. *Blood.* 1984;63(4):917-920.
39. Dominici M, Rasini V, Bussolari R, et al. Restoration and reversible expansion of the osteoblastic hematopoietic stem cell niche after marrow radioablation. *Blood.* 2009;114(11): 2333-2343.
40. Till JE, McCulloch EA. A direct measurement of the radiation sensitivity of normal mouse bone marrow cells. *Radiat Res.* 1961;14:213-222.
41. Fliedner TM, Graessle D, Meineke V, Dörr H. Pathophysiological principles underlying the blood cell concentration responses used to assess the severity of effect after accidental whole-body radiation exposure: an essential basis for an evidence-based clinical triage. *Exp Hematol.* 2007;35(4 Suppl 1):8-16.
42. Peslak SA, Wenger J, Bemis JC, et al. Sublethal radiation injury uncovers a functional transition during erythroid maturation. *Exp Hematol.* 2011; 39(4):434-445.
43. Sugrue T, Lowndes NF, Ceredig R. Mesenchymal stromal cells: radio-resistant members of the bone marrow. *Immunol Cell Biol.* 2013;91(1):5-11.
44. Yamazaki K, Allen TD. Ultrastructural and morphometric alterations in bone marrow stromal tissue after 7 Gy irradiation. *Blood Cells.* 1991; 17(3):527-549.
45. Hooper AT, Butler JM, Nolan DJ, et al. Engraftment and reconstitution of hematopoiesis is dependent on VEGFR2-mediated regeneration of sinusoidal endothelial cells. *Cell Stem Cell.* 2009;4(3):263-274.
46. Ponomaryov T, Peled A, Petit I, et al. Induction of the chemokine stromal-derived factor-1 following DNA damage improves human stem cell function. *J Clin Invest.* 2000;106(11):1331-1339.
47. Olson TS, Caselli A, Otsuru S, et al. Megakaryocytes promote murine osteoblastic HSC niche expansion and stem cell engraftment after radioablative conditioning. *Blood.* 2013; 121(26):5238-5249.
48. Peslak SA, Wenger J, Bemis JC, et al. EPO-mediated expansion of late-stage erythroid progenitors in the bone marrow initiates recovery from sublethal radiation stress. *Blood.* 2012; 120(12):2501-2511.
49. Palis J, Koniski A. Analysis of hematopoietic progenitors in the mouse embryo. *Methods Mol Med.* 2005;105:289-302.

50. Niswander LM, McGrath KE, Kennedy JC, Palis J. Improved quantitative analysis of primary bone marrow megakaryocytes utilizing imaging flow cytometry. *Cytometry A.* 2014;85(4):302-312.
51. McGrath KE, Koniski AD, Maltby KM, McGann JK, Palis J. Embryonic expression and function of the chemokine SDF-1 and its receptor, CXCR4. *Dev Biol.* 1999;213(2):442-456.
52. Palis J, Kingsley PD. Differential gene expression during early murine yolk sac development. *Mol Reprod Dev.* 1995;42(1):19-27.
53. McGrath KE, Frame JM, Fromm GJ, et al. A transient definitive erythroid lineage with unique regulation of the β-globin locus in the mammalian embryo. *Blood.* 2011;117(17):4600-4608.
54. Kowalska MA, Ratajczak J, Hoxie J, et al. Megakaryocyte precursors, megakaryocytes and platelets express the HIV co-receptor CXCR4 on their surface: determination of response to stromal-derived factor-1 by megakaryocytes and platelets. *Br J Haematol.* 1999;104(2):220-229.
55. Ault KA. Reticulated platelets: the birth of a new test for thrombopoiesis. Clin Appl Immunol Rev. 1997;17(1):2-7.
56. Robinson M, MacHin S, Mackie I, Harrison P. In vivo biotinylation studies: specificity of labelling of reticulated platelets by thiazole orange and mepacrine. *Br J Haematol.* 2000;108(4):859-864.
57. Kopp HG, Avecilla ST, Hooper AT, Rafii S. The bone marrow vascular niche: home of HSC differentiation and mobilization. *Physiology (Bethesda).* 2005;20(5):349-356.
58. Kukreja P, Abdel-Mageed AB, Mondal D, Liu K, Agrawal KC. Up-regulation of CXCR4 expression in PC-3 cells by stromal-derived factor-1alpha (CXCL12) increases endothelial adhesion and transendothelial migration: role of MEK/ERK signaling pathway-dependent NF-kappaB activation. *Cancer Res.* 2005;65(21):9891-9898.
59. Gomes AL, Carvalho T, Serpa J, Torre C, Dias S. Hypercholesterolemia promotes bone marrow cell mobilization by perturbing the SDF-1:CXCR4 axis. *Blood.* 2010;115(19):3886-3894.
60. Signoret N, Oldridge J, Pelchen-Matthews A, et al. Phorbol esters and SDF-1 induce rapid endocytosis and down modulation of the chemokine receptor CXCR4. *J Cell Biol.* 1997; 139(3):651-664.
61. Alsayed Y, Ngo H, Runnels J, et al. Mechanisms of regulation of CXCR4/SDF-1 (CXCL12)-dependent migration and homing in multiple myeloma. *Blood.* 2007;109(7):2708-2717.
62. Dar A, Goichberg P, Shinder V, et al. Chemokine receptor CXCR4-dependent internalization and resecretion of functional chemokine SDF-1 by bone marrow endothelial and stromal cells. *Nat Immunol.* 2005;6(10):1038-1046.
63. Laguri C, Arenzana-Seisdedos F, Lortat-Jacob H. Relationships between glycosaminoglycan and receptor binding sites in chemokines-the CXCL12 example. *Carbohydr Res.* 2008;343(12): 2018-2023.
64. Antonsson B, De Lys P, Dechavanne V, Chevalet L, Boschert U. In vivo processing of CXCL12α/SDF-1α after intravenous and subcutaneous administration to mice. *Proteomics.* 2010;10(24): 4342-4351.
65. Rahfeld J, Schierhorn M, Hartrodt B, Neubert K, Heins J. Are diprotin A (Ile-Pro-Ile) and diprotin B (Val-Pro-Leu) inhibitors or substrates of dipeptidyl peptidase IV? *Biochim Biophys Acta.* 1991; 1076(2):314-316.
66. Pereira DA, Gomes L, El-Cheikh MC, Borojevic R. Dipeptidyl peptidase IV (CD26) activity in the hematopoietic system: differences between the membrane-anchored and the released enzyme activity. *Braz J Med Biol Res.* 2003;36(5): 567-578.
67. Lambeir AM, Proost P, Durinx C, et al. Kinetic investigation of chemokine truncation by CD26/dipeptidyl peptidase IV reveals a striking selectivity within the chemokine family. *J Biol Chem.* 2001;276(32):29839-29845.
68. Christopherson KW II, Hangoc G, Broxmeyer HE. Cell surface peptidase CD26/dipeptidylpeptidase IV regulates CXCL12/stromal cell-derived factor-1 alpha-mediated chemotaxis of human cord blood CD34+ progenitor cells. *J Immunol.* 2002; 169(12):7000-7008.
69. Ellis SL, Grassinger J, Jones A, et al. The relationship between bone, hemopoietic stem cells, and vasculature. *Blood.* 2011;118(6): 1516-1524.
70. Neelis KJ, Visser TP, Dimjati W, et al. A single dose of thrombopoietin shortly after myelosuppressive total body irradiation prevents pancytopenia in mice by promoting short-term multilineage spleen-repopulating cells at the transient expense of bone marrow-repopulating cells. *Blood.* 1998;92(5):1586-1597.
71. Arnold JT, Daw NC, Stenberg PE, Jayawardene D, Srivastava DK, Jackson CW. A single injection of pegylated murine megakaryocyte growth and development factor (MGDF) into mice is sufficient to produce a profound stimulation of megakaryocyte frequency, size, and ploidization. *Blood.* 1997;89(3):823-833.
72. Hodohara K, Fujii N, Yamamoto N, Kaushansky K. Stromal cell-derived factor-1 (SDF-1) acts together with thrombopoietin to enhance the development of megakaryocytic progenitor cells (CFU-MK). *Blood.* 2000;95(3):769-775.
73. Guerriero R, Mattia G, Testa U, et al. Stromal cell-derived factor 1alpha increases polyploidization of megakaryocytes generated by human hematopoietic progenitor cells. *Blood.* 2001;97(9):2587-2595.
74. Balduini A, Pallotta I, Malara A, et al. Adhesive receptors, extracellular proteins and myosin IIA orchestrate proplatelet formation by human megakaryocytes. *J Thromb Haemost.* 2008;6(11): 1900-1907.
75. Umezawa H, Aoyagi T, Ogawa K, Naganawa H, Hamada M, Takeuchi T. Diprotins A and B, inhibitors of dipeptidyl aminopeptidase IV, produced by bacteria. *J Antibiot (Tokyo).* 1984; 37(4):422-425.
76. Kawai T, Choi U, Liu P-C, Whiting-Theobald NL, Linton GF, Malech HL. Diprotin A infusion into nonobese diabetic/severe combined immunodeficiency mice markedly enhances engraftment of human mobilized CD34+ peripheral blood cells. *Stem Cells Dev.* 2007; 16(3):361-370.
77. Zaruba M-M, Theiss HD, Vallaster M, et al. Synergy between CD26/DPP-IV inhibition and G-CSF improves cardiac function after acute myocardial infarction. *Cell Stem Cell.* 2009;4(4): 313-323.
78. Theiss HD, Vallaster M, Rischpler C, et al. Dual stem cell therapy after myocardial infarction acts specifically by enhanced homing via the SDF-1/CXCR4 axis. *Stem Cell Res (Amst).* 2011;7(3): 244-255.
79. Broxmeyer HE, Hoggatt J, O'Leary HA, et al. Dipeptidylpeptidase 4 negatively regulates colony-stimulating factor activity and stress hematopoiesis. *Nat Med.* 2012;18(12):1786-1796.
80. Kidd S, Bueso-Ramos C, Jagan S, et al. In vivo expansion of the megakaryocyte progenitor cell population in adult CD26-deficient mice. *Exp Hematol.* 2011;39(5):580-590.e1.
81. Busillo JM, Benovic JL. Regulation of CXCR4 signaling. *Biochim Biophys Acta.* 2007;1768(4): 952-963.
82. Kollet O, Petit I, Kahn J, et al. Human CD34(+) CXCR4(-) sorted cells harbor intracellular CXCR4, which can be functionally expressed and provide NOD/SCID repopulation. *Blood.* 2002; 100(8):2778-2786.
83. Speth JM, Hoggatt J, Singh P, Pelus LM. Pharmacologic increase in HIF1α enhances hematopoietic stem and progenitor homing and engraftment. *Blood.* 2014;123(2):203-207.
84. Ceradini DJ, Kulkarni AR, Callaghan MJ, et al. Progenitor cell trafficking is regulated by hypoxic gradients through HIF-1 induction of SDF-1. *Nat Med.* 2004;10(8):858-864.
85. Lerman OZ, Greives MR, Singh SP, et al. Low-dose radiation augments vasculogenesis signaling through HIF-1-dependent and -independent SDF-1 induction. *Blood.* 2010; 116(18):3669-3676.
86. Zweegman S, Kessler FL, Celie JWAM, et al. Restoration of the human stem cell niche after stem cell transplantation. *Blood.* 2009;114(26): 5404-5406, author reply 5406-5407.
87. Caselli A, Olson TS, Otsuru S, et al. IGF-1-mediated osteoblastic niche expansion enhances long-term hematopoietic stem cell engraftment after murine bone marrow transplantation. *Stem Cells.* 2013;31(10):2193-2204.
88. Sugrue T, Brown JAL, Lowndes NF, Ceredig R. Multiple facets of the DNA damage response contribute to the radioresistance of mouse mesenchymal stromal cell lines. *Stem Cells.* 2013;31(1):137-145.
89. Tzeng YS, Li H, Kang YL, Chen WC, Cheng WC, Lai DM. Loss of Cxcl12/Sdf-1 in adult mice decreases the quiescent state of hematopoietic stem/progenitor cells and alters the pattern of hematopoietic regeneration after myelosuppression. *Blood.* 2011;117(2):429-439.
90. Nombela-Arrieta C, Pivarnik G, Winkel B, et al. Quantitative imaging of haematopoietic stem and progenitor cell localization and hypoxic status in the bone marrow microenvironment. *Nat Cell Biol.* 2013;15(5):533-543.
91. Kunisaki Y, Bruns I, Scheiermann C, et al. Arteriolar niches maintain haematopoietic stem cell quiescence. *Nature.* 2013;502(7473): 637-643.
92. Wang B, Nichol JL, Sullivan JT. Pharmacodynamics and pharmacokinetics of AMG 531, a novel thrombopoietin receptor ligand. *Clin Pharmacol Ther.* 2004;76(6):628-638.
93. Jenkins JM, Williams D, Deng Y, et al. Phase 1 clinical study of eltrombopag, an oral, nonpeptide thrombopoietin receptor agonist. *Blood.* 2007; 109(11):4739-4741.